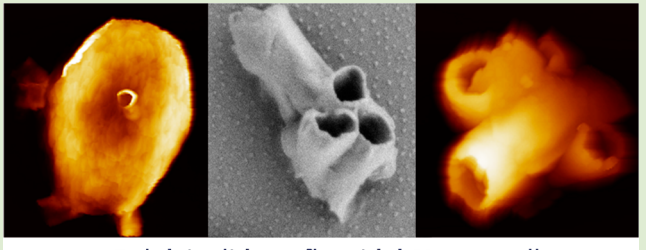
Structure and Morphology of Poly(vinylidene fluoride) Nanoscrolls

Gabriel R. Burks, Hao Qi, Sarah E. Gleeson, Shan Mei, and Christopher Y. Li*

Department of Materials Science and Engineering, Drexel University, Philadelphia, Pennsylvania 19104, United States

Supporting Information

ABSTRACT: To date the scrolled morphology of γ -phase poly(vinylidene fluoride) (PVDF) has been witnessed via high temperature melt crystallization of crystalline thin films and through imaging of chemical etched PVDF bulk films. Here we show the first growth and characterization of free-standing γ phase PVDF scrolls via solution crystallization. Scanning electron microscopy, transmission electron microscopy, and atomic force microscopy have been used to characterize and to further understand the fundamental preferred crystalline habit of the γ -phase of PVDF.



Poly(vinylidene fluoride) Nanoscrolls

ver the years there has been much debate surrounding the origin of various polymer lamellar morphologies. While incommensurate with translational symmetry, nonflat twisting, bending, and scrolling crystals are often observed in semicrystalline polymers. The twisted polymer crystal alone highlights a few decades of research. Compared with lamellar twisting, lamellar scrolling behavior occurs less frequently; reported scrolling polymer crystal systems including iPBu-1 in its Form III,² polyamides 6,6,³ branched alkanes,⁴ the γ -phase polymorph of poly(vinylidene fluoride)(PVDF),5 and copolymers.6

Among the previously mentioned scrolling systems, the γ phase of PVDF has been shown to be of great interest because of its potential applications as a functional polymer, inherent complex polymorphism, and its demonstrated transition from a lamellar twisting state (α -phase) to a lamellar scrolling state (γ phase). The γ-phase of PVDF, along with PVDF as a whole, has been studied extensively.⁸ This γ-phase adopts a T³G⁺T³G⁻ molecular conformation, which can be considered as an α - and β -phase conformational intermediate, and possesses a monoclinic unit cell structure with dimensions of $a = 4.96 \text{ Å}, b = 9.67 \text{ Å}, c = 9.20 \text{ Å}, and <math>\beta = 93^{\circ}$, as demonstrated by Takahashi and Tadokoro using X-ray fiber diffraction and Lovinger using selected area electron diffraction (SAED), settling many years of crystallographic structural debate.7

The first documented acknowledgment of γ -PVDF adopting a scrolling morphology was presented by Vaughn, 5a while a follow-up assessment and a detailed proposal on the formation mechanism of this scrolling was produced by Lotz et al. 1a,5b Through both accounts, the scrolling habit of γ -PVDF had solely been visualized as a product of high temperature melt crystallization. Figure 1 is a reproduced atomic force microscopy (AFM) image of an etched γ-PVDF spherulite surface from unpublished work of Ivanov. 1a The unusual continuous bending of the lamellae led the authors to conclude that the crystals must be scrolling, as shown in the schematics

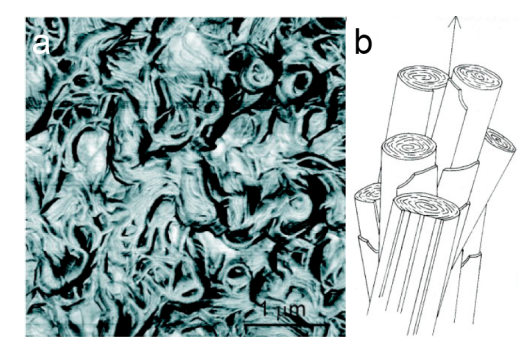


Figure 1. (a) Atomic force microscopy image of γ -phase PVDF as seen down the scroll axis from previous reports. 1a (b) Original schematic representation of nonhollow PVDF scroll by Vaughan.5

in Figure 1b, reproduced from Vaughan.^{5a} It was further pointed out that the scroll axis is the crystallographic b-axis and the scroll diameter varies from submicron to $1-2 \mu m$. ^{1a} As it can be seen in Figure 1, these crystals were viewed from the scroll axis, therefore much of the scroll structure is unclear, particularly the interior regions of the scroll.

Contrarily, solution crystallization typically leads to more well-defined, "clean" polymer single crystals (PSCs). 10 Compared with bulk crystallization, the use of a dilute solution helps to avoid a complex, secondary habit of crystals clustering into dendrites or spherulites that could obscure the primary single crystal growth process. Recent advancements have demonstrated that well-controlled PSCs can find broad applications in nanoparticle synthesis, 11 nanoparticle patterning, 11h,12 carbon nanotube functionalization, 13 nanomotors, surface enhanced Raman spectroscopy, ¹⁵ catalyst supports, ¹⁶ drug delivery and microphage imaging, ¹⁷ Janus sheets and

Received: November 22, 2017 Accepted: December 19, 2017 Published: December 21, 2017

ACS Macro Letters

brush synthesis.¹⁸ Crystallization-induced block copolymer assembly has also been intensively pursued.¹⁹ While solution crystallized PVDF was investigated as early as the 1960s,²⁰ scrolling had not been observed. It is the intention of this work to pursue clean scrolling PVDF single crystals and reveal the detailed growth habits. We envisage that this work would contribute to the broad field of nonflat polymer crystals.

PVDF used in this study was Kynar 740 ($\dot{M}_{\rm w}=156000~{\rm Da}$), supplied by Arkema. For a typical experimental procedure, samples were isothermally crystallized from a 9:1 monochlor-obenzene and N, N-dimethylformamide solvent mixture at 110 °C and allowed to crystallize for 10 h. To avoid the incorporation of overgrowth of free polymer, isothermal filtration was conducted at the crystallization temperature at the conclusion of the crystallization time. PVDF single crystals were obtained at 0.01 wt % polymer concentration. The resulting structures are shown in Figure 2a, where two primary

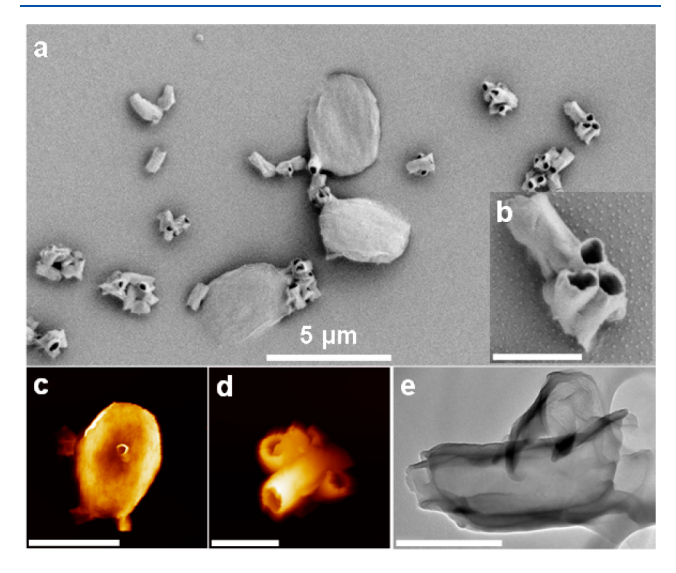


Figure 2. Morphology of PVDF single crystals grown at 0.01 wt % polymer concentration. (a) SEM micrographs of PVDF flat single crystals and nanoscrolls and (b) higher magnification of (a), where the scale bar represents 1 μ m. (c, d) AFM micrographs PVDF flat and scroll single crystals. The scale bars for (c) and (d) represent 3 and 1 μ m, respectively. (e) TEM micrograph show two PVDF nanoscrolls. Note that the upper one is half closed. The scale bar represents 500 nm

crystal morphologies, the faceted flat lamellar crystal and the cylindrical tubes, are identifiable. The tubular objects in Figure 2a are of particular interest. It appears that they have a relatively narrow size distribution (see later discussion) and are free-standing. Figure 2b shows the enlarged SEM micrograph of Figure 2a. Four tubes with submicron diameter seemingly aggregate together, where three tubes are parallel to each other and one is orientated in a nearly orthogonal direction. The opening of the tips are faceted, suggesting the crystalline nature of the objects. These two types of morphologies are also shown with AFM experiments, seen in Figure 2c,d. The surface of the flat faceted crystals is rough, covered with multiple decorated small lamellae. The three-dimensional features of the tubular structure are clearly seen under AFM. These tubular structures are similar to the reported scrolls seen in the γ -form PVDF spherulite (Figure 1), while they seem to have tubular instead of scrolling shape. In our observation, we did occasionally observe curved scrolling objects, as shown in Figure 2e. This

led us to conclude that the tubes in Figure 2 are simply enclosed scrolls, morphologically similar to the scroll crystals previously reported. To adopt a common nomenclature consistent with previous reports, we shall further refer to the cylindrical tubes as scrolls.

To identify the phase structure of these two crystalline morphologies, TEM SAED was used, and the results are shown in Figure 3, while a lower magnification TEM micrograph is

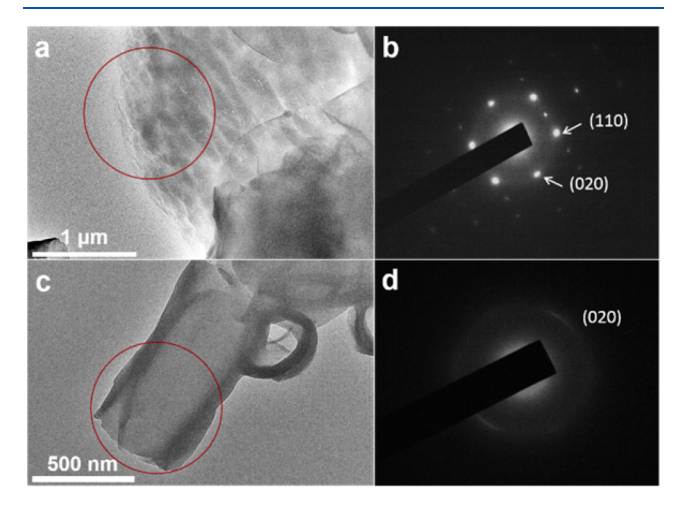


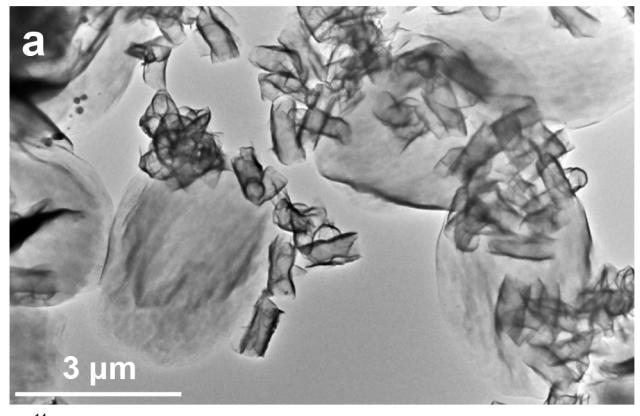
Figure 3. (a) TEM image and (b) corresponding SAED of PVDF faceted PVDF flat crystals. (c) TEM image and (d) corresponding SAED of PVDF nanoscrolls.

shown in Figure 4a. TEM micrographs of the flat faceted crystals (Figure 3a) show that their surface is decorated with numerous small overgrown lamellar crystals, consistent with AFM observation (Figure 2c). A strong SAED pattern was recorded (Figure 3b) with correct orientation with Figure 3a. The diffraction pattern indicates that these faceted crystals are from PVDF α -phase. However, the diffraction from the scroll crystals is much weaker whereby only a pair of faint arcs are observed. This diffraction pair can be assigned as (020) based on the γ-phase PVDF crystalline structure. The weak and arcshaped diffraction can be attributed to the continuous curving nature of the crystal and the small corresponding geometric area (much smaller than the selected area) of lamellar planes contributing to the diffraction signal. This is in drastic contrast to the diffraction pattern from the flat α -phase PVDF crystal (Figure 3b), where strong and sharp diffraction spots can be easily identified because the entire selected area contributes to the diffraction pattern. Similar behaviors have been observed in helical crystals and most recently in polymer crystalsomes.²¹ Our observed orientation of the (020) also suggests that the scroll axis is along the [020] direction of the lattice, consistent with previous literature. 1a

Compared with previously observed γ -form PVDF scroll crystals, the present work shows for the first time isolated, individual PVDF nanoscrolls. A few key characteristics can be concluded by comparing Figures 1 and 2: (1) the scrolls are of hollow nature, contrary to previous schematic representations shown in Figure 1, (2) the PVDF scrolls possess a uniform size distribution. Figure 4a is a low magnification TEM image of the nanoscrolls, and Figure 4b shows the histogram of the scroll diameter and length based on Figure 4a. All the scrolls are \sim 310–520 nm in diameter, and \sim 1 μ m in length, much more uniform compared with the melt crystallized samples. (3)

ACS Macro Letters

Letter



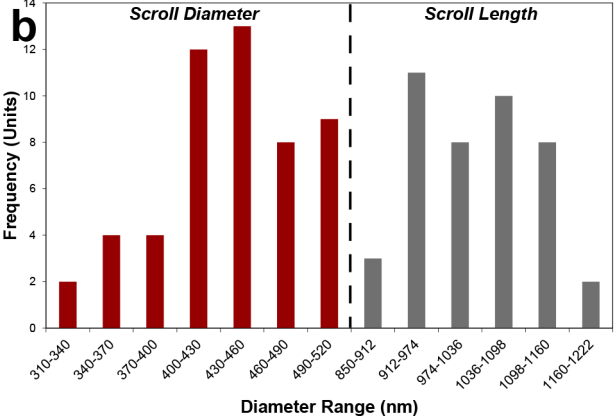


Figure 4. (a) Low magnification TEM micrograph of PVDF scrolls, scroll clusters, and alpha crystals. (b) Histogram indicating the relative scroll diameters and lengths.

SEM and TEM observations suggest that scrolls tend to form clusters, and also have an affinity for the edges and central regions of the flat α phase crystals (Figure 2).

The more isolated structures and uniform size of the nanoscrolls observed in this work may be a product of the dilute solution system used, minimizing the polymer diffusion effect in previous bulk cases. As it relates to the affinity that α and γ -PVDF appear to have for another, as well as γ -PVDF to itself, one of the more intriguing observations pertains to the resulting orientation of these clustered crystals. As it can be seen in Figures 2b,c and 3c, the scrolls have a tendency to grow in such an orientation where the b-axis is perpendicular to the lamellar surface of the α -phase and both parallel and perpendicular to the b-axis of other scrolls. The orthogonal orientation of the adjacent scrolls seen in Figures 2b and 3c can be attributed to the small lattice mismatching (Δ) between (020) $\gamma/(100)$ γ ($\Delta \sim 2.4\%$). The overgrowth of the γ -scroll on the flat α -crystals is perhaps due to the close lattice matching between (010) $\gamma/(001)$ γ ($\Delta \sim 5\%$), and between (010) $\alpha/(010)$ γ ($\Delta \sim 0.3\%$). Such close lattice parameters between the two phases, and between the a- and b-axis of each phase brings about the possibility of observed overgrowth.

The mechanism of PVDF scrolling has been proposed by Lotz et al. The idea can be summarized as follows. The γ -PVDF unit cell is polar with a specific chain orientation, which directly leads to an odd number of carbon atoms in each fold. Assuming nine backbone carbons per fold, this leads to the "asymmetric folding" with a 4CH₂/5CF₂ and 5CH₂/4CF₂ on the opposite sides of the γ -PVDF crystal. The relative difference in volume (~355 vs 345 ų) was believed to

cause a $\sim 0.04^\circ$ splaying angle per chain, resulting in a scrolled crystal with a radius of $\sim 1-2~\mu m.^{1a,Sb}$ Note that in the previous SEM and AFM reports, viewed from the spherulite surface, the scroll morphology is less defined. In the present case, the well-defined, isolated scroll morphology allows us to conduct a more detailed calculation.

Starting from the average diameter of 400 nm, since the scrolling axis is b, each layer of the PVDF chain along the tangential direction splays $\sim\!\Delta\theta=\frac{360\times a}{2\pi r}$, where a is the unit cell a-axis of PVDF (0.495 nm), r is the scroll radius (200 nm). Plugging the a and r values into the equation leads to a splay angle of 0.14°, slightly higher than the previous value, which is due to the smaller diameter of the scrolls observed in our case.

We can look into the origin of this splay in more detail as shown in Figure 5c. Each chain in the crystal can be viewed as

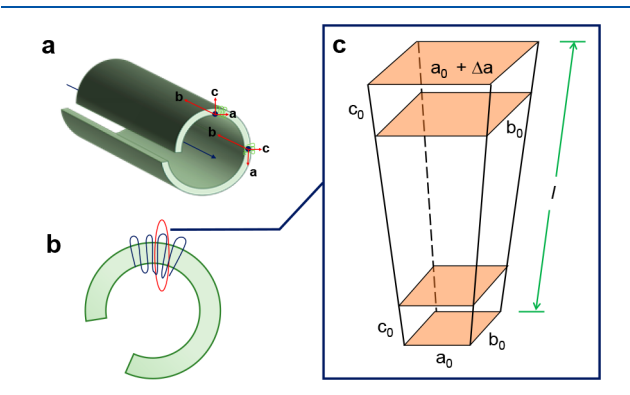


Figure 5. PVDF scroll schematic indicating the scrolled crystals and the chain folding. (a, b) PVDF scroll viewed from side (a) and scroll axis (b) directions. (c) Schematics showing the imbalanced folding.

three sections: those contributing to either the top or the bottom fold surfaces, and one straight crystalline stem. We assume the total thickness of the crystal is l, the inner fold volume can be viewed as $V_{\text{inner}} = a_0 \times b_0 \times c_0$, where a_0 , b_0 , and c_0 represent the dimension of the inner fold (inner crystal surface in the scroll) along the crystallographic a, b, and c directions. For the outer fold volume, since the scroll axis is b, the b-dimension should be similar to b_0 , otherwise, biaxial bending would occur. It is unclear if the c dimension changes, and for the ease of calculation, we assume it does not. The outer fold volume can therefore be expressed as $V_{\text{outer}} = (a_0 +$ Δa) × b_0 × c_0 , where Δa is the distortion of the lattice along a direction, which eventually leads to scrolling. Consider l is 10 nm, for a scroll with r = 200 nm, Δa is ~ 0.24 Å. This directly led to the volume mismatch to be $\sim \tilde{V} = V_{\rm outer}/V_{\rm inner} = 1.05$. Recalling that the nine-carbon folding leads to a volume mismatch of $\sim \tilde{V} = 355 \text{ Å}^3/345 \text{ Å}^3 = \sim 1.03$. Since there are two stems involved in one fold, the true volume mismatch per stem is therefore 1.015, which is slightly smaller than the calculated 1.05 based on the morphological observation.

The slight discrepancy could arise from (1) the true shape of the fold volume might be anisotropic along the a- and b-axis; (2) it might take less than nine carbon atoms to form a fold, for example, assuming that seven carbon folds will lead to $\tilde{V} \approx 1.04$; (3) possible chain tilting in the crystal might affect the scrolling behavior. It has been pointed out that in the melt grown γ -PVDF single crystals that the chain tilts about 28.5° toward the a-axis, 5b leading to a (104) fold surface. Similar to the case of polyethylene, this chain tilting could affect the chain

ACS Macro Letters

Letter

splay since additional stress is introduced due to chain tilting. ^{1a} Secondarily, it is worth noting that chain tilting was observed in melt grown α -PVDF; while in the case of solution grown α -PVDF, it has been shown that the polymer chain is orthogonal to the lamellar surface. ^{8b,20a} It is unclear if additional chain tilting occurs in the present scrolled crystals due to weak SAED.

In summary, we have grown and characterized isolated free-standing γ -PVDF nanoscrolls via solution crystallization. The natural habit of this scrolled polymer is to form a hollow tubular structure. The reported nanoscrolls are uniform in size, $\sim 310-520$ nm in diameter, and $\sim 1~\mu m$ in length. SAED confirms that the scroll axis is b. A 0.14° splay per molecular layer along the scroll tangential direction (a) can be calculated. Differences in basal surface fold volumes are considered as the main reason for lamellar scrolling, similar to the behavior seen in other previously mentioned scrolling systems. We anticipate that the evolution of this polymer system will further validate the rationale for the formation of scrolling of polymer crystalline lamella.

ASSOCIATED CONTENT

Supporting Information

The Supporting Information is available free of charge on the ACS Publications website at DOI: 10.1021/acsmacrolett.7b00921.

Experimental details (PDF).

AUTHOR INFORMATION

Corresponding Author

*E-mail: chrisli@drexel.edu.

ORCID ®

Christopher Y. Li: 0000-0003-2431-7099

Author Contributions

The manuscript was written through contributions of all authors. All authors have given approval to the final version of the manuscript.

Notes

The authors declare no competing financial interest.

ACKNOWLEDGMENTS

This work was supported by the National Science Foundation Grant DMR-1709136.

■ REFERENCES

- (1) (a) Lotz, B.; Cheng, S. Z. D. A critical assessment of unbalanced surface stresses as the mechanical origin of twisting and scrolling of polymer crystals. *Polymer* **2005**, *46*, 577–610. (b) Keith, H. D.; Padden, F. J. Banding in polyethylene and other spherulites. *Macromolecules* **1996**, *29*, 7776–7786. (c) Crist, B.; Schultz, J. M. Polymer spherulites: A critical review. *Prog. Polym. Sci.* **2016**, *56*, 1–63. (d) Bassett, D. C. Polymer spherulites: A modern assessment. *J. Macromol. Sci., Part B: Phys.* **2003**, *42*, 227–256. (e) Toda, A.; Taguchi, K.; Hikosaka, M.; Kajioka, H. Branching and Higher Order Structure in Banded Poly(vinylidene fluoride) Spherulites. *Polym. J.* **2008**, *40*, 905–909. (f) Wen, T.; Shen, H. Y.; Wang, H. F.; Mao, Y. C.; Chuang, W. T.; Tsai, J. C.; Ho, R. M. Controlled Handedness of Twisted Lamellae in Banded Spherulites of Isotactic Poly(2-vinylpyridine) as Induced by Chiral Dopants. *Angew. Chem., Int. Ed.* **2015**, *54*, 14313–14316.
- (2) (a) Holland, V. F.; Miller, L. M. Isotactic Polybutene-1 Single Crystals: Morphology. *J. Appl. Phys.* **1964**, *35*, 3241–3248. (b) Khoury, F.; Barnes, J. D. Formation of curved polymer crystals

- poly(4-methylpentene-1). J. Res. Natl. Bur. Stand., Sect. A 1972, 76A, 225–252.
- (3) (a) Geil, P. H. Nylon single crystals. *J. Polym. Sci.* **1960**, *44*, 449–458. (b) Cai, W. W.; Li, C. Y.; Li, L. Y.; Lotz, B.; Keating, M. N.; Marks, D. Submicrometer scroll/tubular lamellar crystals of Nylon *6*,*6*. *Adv. Mater.* **2004**, *16*, 600–605.
- (4) (a) White, H. M.; Hosier, I. L.; Bassett, D. C. Cylindrical lamellar habits in monodisperse centrally branched alkanes. *Macromolecules* **2002**, *35*, 6763–6765. (b) Rhodes, F. H.; Mason, C. W.; Sutton, W. R. Crystallization of Paraffin Wax1. *Ind. Eng. Chem.* **1927**, *19*, 935–938.
- (5) (a) Vaughan, A. S. Etching and Morphology of Poly(Vinylidene Fluoride). *J. Mater. Sci.* **1993**, 28, 1805–1813. (b) Lotz, B.; Thierry, A.; Schneider, S. Molecular origin of the scroll-like morphology of lamellae in gamma PVF2 spherulites. *C. R. Acad. Sci., Ser. IIc: Chim.* **1998**, 1, 609–614.
- (6) (a) Xiong, H. M.; Chen, C. K.; Lee, K.; Van Horn, R. M.; Liu, Z.; Ren, B.; Quirk, R. P.; Thomas, E. L.; Lotz, B.; Ho, R. M.; Zhang, W. B.; Cheng, S. Z. D. Scrolled Polymer Single Crystals Driven by Unbalanced Surface Stresses: Rational Design and Experimental Evidence. *Macromolecules* 2011, 44, 7758–7766. (b) Agbolaghi, S.; Zenoozi, S.; Hosseini, Z.; Abbasi, F. Scrolled/Flat Crystalline Structures of Poly(3-hexylthiophene) and Poly(ethylene glycol) Block Copolymers Subsuming Unseeded Half-Ring-Like and Seeded Cubic, Epitaxial, and Fibrillar Crystals. *Macromolecules* 2016, 49, 9531–9541.
- (7) (a) Osaki, S.; Ishida, Y. Effects of annealing and isothermal crystallization upon crystalline forms of poly(vinylidene fluoride). *J. Polym. Sci., Polym. Phys. Ed.* **1975**, *13*, 1071–1083. (b) Lovinger, A. J. Conformational Defects and Associated Molecular Motions in Crystalline Poly(Vinylidene Fluoride). *J. Appl. Phys.* **1981**, *52*, 5934–5938. (c) Lovinger, A. J. Ferroelectric polymers. *Science* **1983**, *220*, 1115–1121.
- (8) (a) Lovinger, A. J.; Keith, H. D. Electron Diffraction Investigation of a High-Temperature Form of Poly(vinylidene fluoride). *Macromolecules* 1979, 12, 919–924. (b) Lovinger, A. J. Polyvinylidene fluoride. In *Developments in Crystalline Polymers* 1, Bassett, D. C., Ed.; Springer Science & Business Media, 1982; Vol. 33, pp 195–262.
- (9) (a) Lovinger, A. J. Unit-Cell of the Gamma-Phase of Poly(Vinylidene Fluoride). *Macromolecules* **1981**, *14*, 322–325. (b) Lovinger, A. J. Crystalline Transformations in Spherulites of Poly(Vinylidene Fluoride). *Polymer* **1980**, *21*, 1317–1322. (c) Takahashi, Y.; Tadokoro, H. Formation Mechanism of Kink Bands in Modification-Ii of Poly(Vinylidene Fluoride) Evidence for Flip-Flop Motion between Tgtg-Bar and Tg-Bartg Conformations. *Macromolecules* **1980**, *13*, 1316–1317.
- (10) Geil, P. H. *Polymer Single Crystals*; Interscience Publishers, 1963; p 560.
- (11) (a) Li, B.; Ni, C.; Li, C. Y. Poly(ethylene oxide) single crystals as templates for Au nanoparticle patterning and asymmetrical functionalization. Macromolecules 2008, 41, 149-155. (b) Wang, B. B.; Li, B.; Zhao, B.; Li, C. Y. Amphiphilic Janus gold nanoparticles via combining "Solid-State Grafting-to" and "Grafting-from" methods. J. Am. Chem. Soc. 2008, 130, 11594-11595. (c) Li, B.; Li, L. Y.; Wang, B. B.; Li, C. Y. Alternating patterns on single-walled carbon nanotubes. Nat. Nanotechnol. 2009, 4, 358-362. (d) Li, B.; Wang, B. B.; Ferrier, R. C. M.; Li, C. Y. Programmable Nanoparticle Assembly via Polymer Single Crystals. Macromolecules 2009, 42, 9394-9399. (e) Li, C. Y. Polymer single crystal meets nanoparticles. J. Polym. Sci., Part B: Polym. Phys. 2009, 47, 2436-2440. (f) Li, B.; Li, C. Y. Immobilizing Au nanoparticles with polymer single crystals, patterning and asymmetric functionalization. J. Am. Chem. Soc. 2007, 129, 12-13. (g) Wang, B. B.; Dong, B.; Li, B.; Zhao, B.; Li, C. Y. Janus gold nanoparticle with bicompartment polymer brushes templated by polymer single crystals. Polymer 2010, 51, 4814-4822. (h) Wang, B. B.; Li, B.; Dong, B.; Zhao, B.; Li, C. Y. Homo- and Hetero-Particle Clusters Formed by Janus Nanoparticles with Bicompartment Polymer Brushes. Macromolecules 2010, 43, 9234-

ACS Macro Letters

Letter

9238. (i) Wang, B. B.; Li, B.; Ferrier, R. C. M.; Li, C. Y. Polymer Single Crystal Templated Janus Nanoparticles. *Macromol. Rapid Commun.* 2009, 31, 169–175. (j) Dong, B.; Li, B.; Li, C. Y. Janus nanoparticle dimers and chains via polymer single crystals. *J. Mater. Chem.* 2011, 21, 13155–13158. (k) Zhou, T.; Wang, B.; Dong, B.; Li, C. Y. Thermoresponsive Amphiphilic Janus Silica Nanoparticles via Combining "Polymer Single-Crystal Templating" and "Graftingfrom" Methods. *Macromolecules* 2012, 45, 8780–8789. (l) Zhou, T.; Dong, B.; Qi, H.; Lau, H. K.; Li, C. Y. One-step formation of responsive "dumbbell" nanoparticle dimers via quasi-two-dimensional polymer single crystals. *Nanoscale* 2014, 6, 4551–4554. (m) Zhou, T.; Dong, B.; Qi, H.; Mei, S.; Li, C. Y. Janus hybrid hairy nanoparticles. *J. Polym. Sci., Part B: Polym. Phys.* 2014, 52, 1620–1640.

- (12) (a) Zhang, H.; Dong, B.; Zhou, T.; Li, C. Y. Directed Self-assembly of Hetero-Nanoparticles Using Polymer Single Crystal Template. *Nanoscale* **2012**, *4*, 7641–7645. (b) Mei, S.; Qi, H.; Zhou, T.; Li, C. Y. Precisely Assembled Cyclic Gold Nanoparticle Frames by 2D Polymer Single-Crystal Templating. *Angew. Chem., Int. Ed.* **2017**, 56, 1–6.
- (13) (a) Laird, E. D.; Li, C. Y. Structure and Morphology Control in Crystalline-Polymer/Carbon-Nanotube Composites. *Macromolecules* **2013**, *46*, 2877–2891. (b) Li, C. Y.; Li, L.; Cai, W.; Kodjie, S. L.; Tenneti, K. K. Nanohybrid shish-kebabs: periodically functionalized carbon nanotubes. *Adv. Mater.* **2005**, *17*, 1198–1202. (c) Li, L.; Li, C. Y.; Ni, C. Y. Polymer crystallization-driven, periodic patterning on carbon nanotubes. *J. Am. Chem. Soc.* **2006**, *128*, 1692–1699. (d) Wang, W.; Li, C. Y. Single-Walled Carbon Nanotube-Induced Orthogonal Growth of Polyethylene Single Crystals at a Curved Liquid/Liquid Interface. *ACS Macro Lett.* **2014**, *3*, 175–179. (e) Wang, W.; Huang, Z.; Laird, E. D.; Wang, S.; Li, C. Y. Single-walled carbon nanotube nanoring induces polymer crystallization at liquid/liquid interface. *Polymer* **2015**, *59*, 1–9.
- (14) (a) Dong, B.; Zhou, T.; Zhang, H.; Li, C. Y. Directed Self-Assembly of Nanoparticles for Nanomotors. *ACS Nano* **2013**, *7*, 5192–5198. (b) Liu, M.; Liu, L. M.; L, G. W.; Su, M. D.; Ge, Y.; Shi, L. L.; Zhang, H.; Dong, B.; Li, C. Y. A micromotor based on polymer single crystals and nanoparticles: toward functional versatility. *Nanoscale* **2014**. *6*. 8601–8605.
- (15) Dong, B.; Wang, W.; Miller, D. L.; Li, C. Y. Polymer-single-crystal@nanoparticle nanosandwich for surface enhanced Raman spectroscopy. *J. Mater. Chem.* **2012**, 22, 15526–15529.
- (16) Dong, B.; Miller, D. L.; Li, C. Y. Polymer Single Crystal As Magnetically Recoverable Support for Nanocatalysts. *J. Phys. Chem. Lett.* **2012**, *3*, 1346–1350.
- (17) Zhu, W.; Peng, B.; Wang, J.; Zhang, K.; Liu, L.; Chen, Y. Bamboo Leaf-Like Micro-Nano Sheets Self-Assembled by Block Copolymers as Wafers for Cells. *Macromol. Biosci.* **2014**, *14*, 1764–1770.
- (18) (a) Qi, H.; Wang, W.; Li, C. Y. Janus Polymer Single Crystal via Evaporative Crystallization. *ACS Macro Lett.* **2014**, *3*, 675–678. (b) Qi, H.; Zhou, T.; Mei, S.; Chen, X.; Li, C. Y. Responsive Shape Change of Sub-5 nm Thin, Janus Polymer Nanoplates. *ACS Macro Lett.* **2016**, *5*, 651–655. (c) Zhou, T.; Qi, H.; Han, L.; Barbash, D.; Li, C. Y. Towards controlled polymer brushes via a self-assembly-assisted-grafting-to approach. *Nat. Commun.* **2016**, *7*, 11119.
- (19) (a) Lotz, B.; Kovacs, A. J. Propriétés des copolymères biséquencés polyoxyéthylène-polystyrène I. Préparation, composition et étude microscopique des monocristaux. *Kolloid Z. Z. Polym.* 1966, 209, 97. (b) Chen, W. Y.; Li, C. Y.; Zheng, J. X.; Huang, P.; Zhu, L.; Ge, Q.; Quirk, R. P.; Lotz, B.; Deng, L. F.; Wu, C.; Thomas, E. L.; Cheng, S. Z. D. "Chemically shielded" poly(ethylene oxide) single crystal growth and construction of channel-wire arrays with chemical and geometric recognitions on a submicrometer scale. *Macromolecules* 2004, 37, 5292–5299. (c) Chen, W. Y.; Zheng, J. X.; Cheng, S. Z. D.; Li, C. Y.; Huang, P.; Zhu, L.; Xiong, H. M.; Ge, Q.; Guo, Y.; Quirk, R. P.; Lotz, B.; Deng, L. F.; Wu, C.; Thomas, E. L. Onset of tethered chain overcrowding. *Phys. Rev. Lett.* 2004, 93, 1–4. (d) Nazemi, A.; He, X. M.; MacFarlane, L. R.; Harniman, R. L.; Hsiao, M. S.; Winnik, M. A.; Faul, C. F. J.; Manners, I. Uniform "Patchy" Platelets by

Seeded Heteroepitaxial Growth of Crystallizable Polymer Blends in Two Dimensions. *J. Am. Chem. Soc.* **2017**, *139*, 4409–4417. (e) Pitto-Barry, A.; Kirby, N.; Dove, A. P.; O'Reilly, R. K. Expanding the scope of the crystallization-driven self-assembly of polytactide-containing polymers. *Polym. Chem.* **2014**, *5*, 1427–1436.

- (20) (a) Okuda, K.; Yoshida, T.; Sugita, M.; Asahina, M. Solution-grown crystals of poly (vinylidene fluoride). *J. Polym. Sci., Part B: Polym. Lett.* **1967**, *5*, 465–468. (b) Miller, R. L.; Raisoni, J. Single crystals of poly (vinylidene fluoride). *J. Polym. Sci., Polym. Phys. Ed.* **1976**, *14*, 2325–2326.
- (21) (a) Li, C. Y.; Cheng, S. Z. D.; Ge, J. J.; Bai, F.; Zhang, J. Z.; Mann, I. K.; Harris, F. W.; Chien, L. C.; Yan, D. H.; He, T. B.; Lotz, B. Double twist in helical polymer "soft" crystals. Phys. Rev. Lett. 1999, 83, 4558-4561. (b) Li, C. Y.; Yan, D. H.; Cheng, S. Z. D.; Bai, F.; Ge, J. J.; Calhoun, B. H.; He, T. B.; Chien, L. C.; Harris, F. W.; Lotz, B. Helical single-lamellar crystals thermotropically formed in a synthetic nonracemic chiral main-chain polyester. Phys. Rev. B: Condens. Matter Mater. Phys. 1999, 60, 12675-12680. (c) Li, C. Y.; Yan, D. H.; Cheng, S. Z. D.; Bai, F.; He, T. B.; Chien, L. C.; Harris, F. W.; Lotz, B. Double-twisted helical lamellar crystals in a synthetic main-chain chiral polyester similar to biological polymers. Macromolecules 1999, 32, 524-527. (d) Li, C. Y.; Cheng, S. Z. D.; Ge, J. J.; Bai, F.; Zhang, J. Z.; Mann, I. K.; Chien, L. C.; Harris, F. W.; Lotz, B. Molecular orientations in flat-elongated and helical lamellar crystals of a main-chain nonracemic chiral polyester. J. Am. Chem. Soc. 2000, 122, 72-79. (e) Li, C. Y.; Ge, J. J.; Bai, F.; Calhoun, B. H.; Harris, F. W.; Cheng, S. Z. D.; Chien, L. C.; Lotz, B.; Keith, H. D. Early-stage formation of helical single crystals and their confined growth in thin film. Macromolecules 2001, 34, 3634-3641. (f) Wang, W.; Qi, H.; Zhou, T.; Mei, S.; Han, L.; Higuchi, T.; Jinnai, H.; Li, C. Y. Highly robust crystalsome via directed polymer crystallization at curved liquid/liquid interface. Nat. Commun. 2016, 7, 10599-10599. (g) Wang, W.; Staub, M. C.; Zhou, T.; Smith, D. M.; Qi, H.; Laird, E. D.; Cheng, S.; Li, C. Y. Polyethylene Nano Crystalsome Formed at Curved Liquid/Liquid Interface. Nanoscale 2018, 10, 268-276.